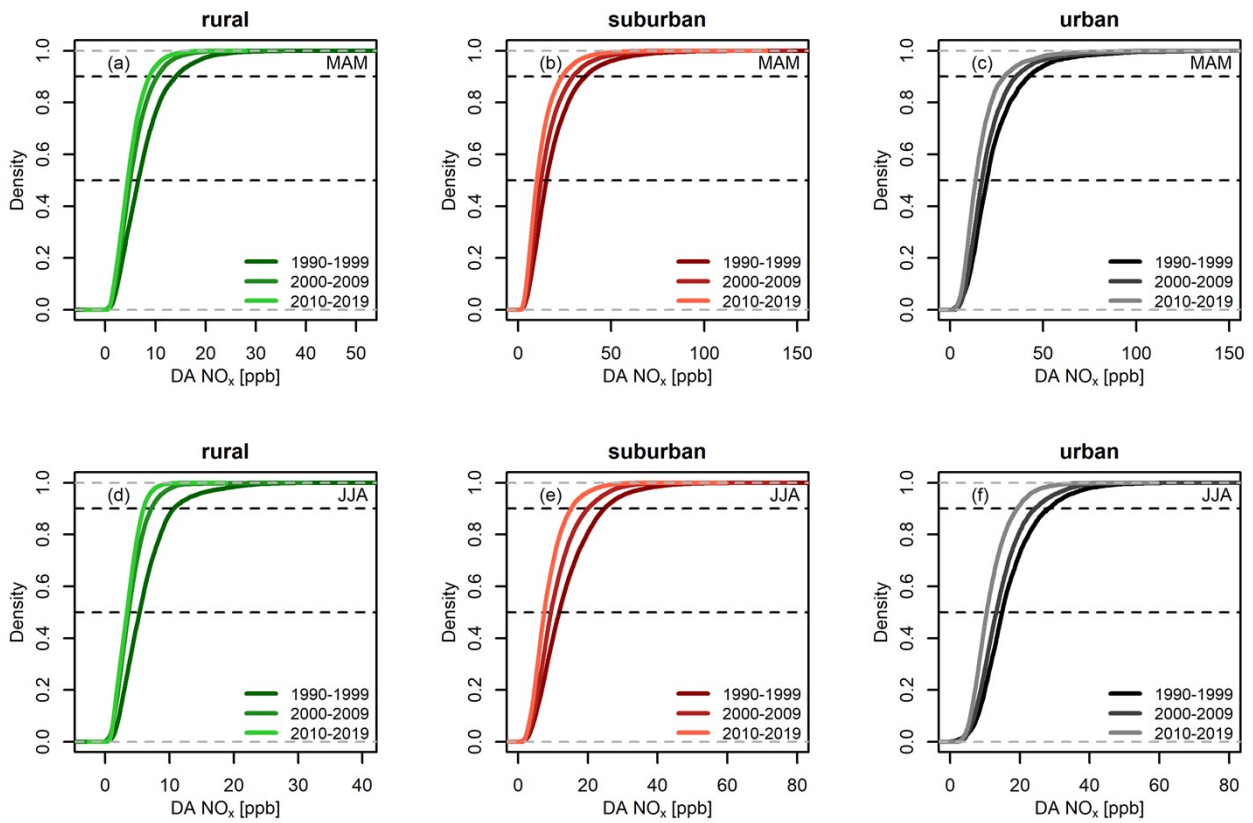


Supplementary information

- 5 **Table S1:** List of O₃ background sites of the Austrian monitoring network used in this study. Station printed in bold provide NO_x observations for the whole study period along with ozone measurements. Sites marked with * indicate the sites selected for representative analysis.

Station name	category	Airbase code	Station name	category	Airbase code
1 Amstetten	urban	AT30101	29 Arnfels	rural	AT60190
2 Graz, Schlossberg	urban	AT60018	30 Dunkelsteinerwald	Rural	AT31701
3 Leoben	urban	AT60143	31 Forsthof am Schöpfl	rural	AT30202
4 Linz, Neue Welt	urban	AT4S416	32 Gänsersdorf	rural	AT30401
5 St. Pölten	urban	AT32301	33 Grundlsee	rural	AT60157
6 Vienna, Stephansplatz*	urban	AT9STEF	34 Haunsberg	rural	AT53055
7 Bad Ischl	suburban	AT4S125	35 Heidenreichstein	rural	AT30502
8 Bad Vöslau - Gainfarn	suburban	AT30201	36 Hochgössnitz	rural	AT60137
9 Eisenstadt	suburban	AT10001	37 Höfen Lärchbichl	rural	AT72705
10 Graz Nord*	suburban	AT60138	38 Illmitz*	rural	AT0ILL1
11 Hainburg	suburban	AT30301	39 Irnfritz	rural	AT30801
12 Innsbruck Sadrach	suburban	AT72113	40 Klöch*	rural	AT60185 (O₃)
13 Judenburg	suburban	AT60018	Klöch*	rural	AT0KLH1(NO_x)
14 Klagenfurt Kreuzbergl	suburban	AT2KA41	41 Kollmitzberg	rural	AT30103
15 Klosterneuburg	suburban	AT30601	42 Kramsach Angerberg	rural	AT72538
16 Lustenau Wiesenrain	suburban	AT80706	43 Masenberg*	rural	AT60156
17 Mödling	suburban	AT31401	44 Mistelbach	rural	AT331301
18 Spittal a.d.Drau	suburban	AT2SP18	45 Obervellach	rural	AT2SP10
19 St. Johann im Pongau	suburban	AT54057	46 Pillersdorf	rural	AT0PIL1
20 Steyr	suburban	AT4S409	47 St. Georgen /Lavanttal	rural	AT2WO35
21 Traun	suburban	AT4S404	48 St. Koloman Kleinhorn	rural	AT52055
22 Vienna, Hermannskogel*	suburban	AT9JAEG	49 Stixneusiedl	rural	AT30302
23 Vienna, Hohe Warte	suburban	AT900ZA	50 Streithofen	rural	AT31904
24 Vienna, Laaer Berg	suburban	AT90LAA	51 Sulzberg - Gmeind	rural	AT80503
25 Vienna, Lobau	suburban	AT90LOB	52 Vorhegg	rural	AT0VOR1
26 Wiener Neustadt	suburban	AT332401	53 Wiesmath	rural	AT32101
27 Wolfsberg	suburban	AT2WO15	54 Wolkersdorf	rural	AT30403
28 Annaberg	rural	AT31102			



10

Figure S1: Empirical cumulative probability distribution functions (ECDFs) of daily average (DA) NO_x concentrations for (a) rural, (b) suburban, and (c) urban sites during spring (MAM). (d)-(f) as (a) – (c) but for summer (JJA). Dashed lines in all panels indicate the 50th and 90th percentiles.

15 **Table S2:** Ratios of selected NO_x percentiles (50% (q50) and 90%(q90)) for spring and summer seasons for different site types for 10 year study periods relative to 1990-1999.

Site category / quantile	MAM 2000-2009	MAM 2010-2019	JJA 2000-2009	JJA 2010-2019
Rural q50	0.76	0.68	0.68	0.63
Suburban q50	0.82	0.66	0.80	0.64
Urban q50	0.87	0.70	0.89	0.70
Rural q90	0.74	0.63	0.67	0.56
Suburban q90	0.82	0.65	0.81	0.62
Urban q90	0.84	0.69	0.86	0.68

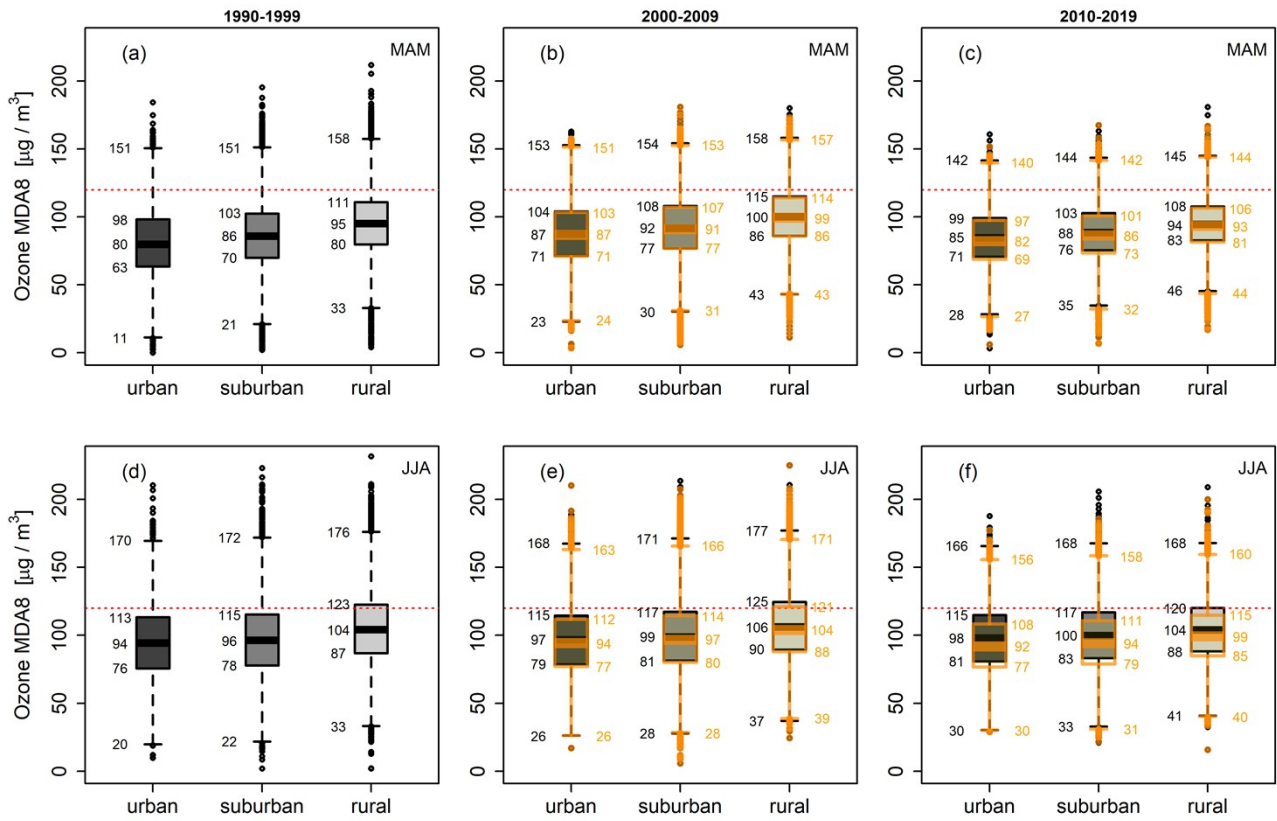


Figure S2: As figure 3 but for MDA8 O₃ concentrations.

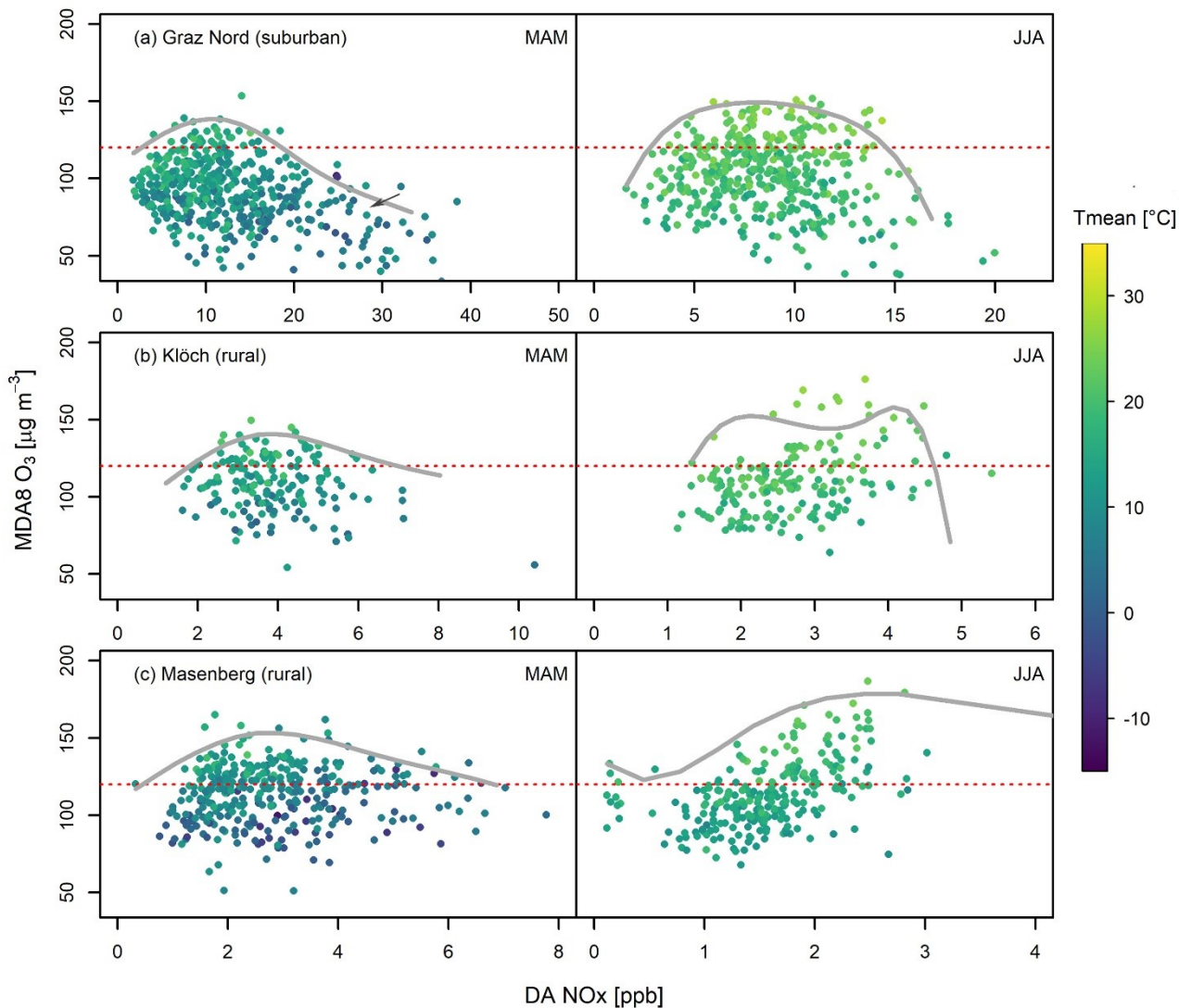
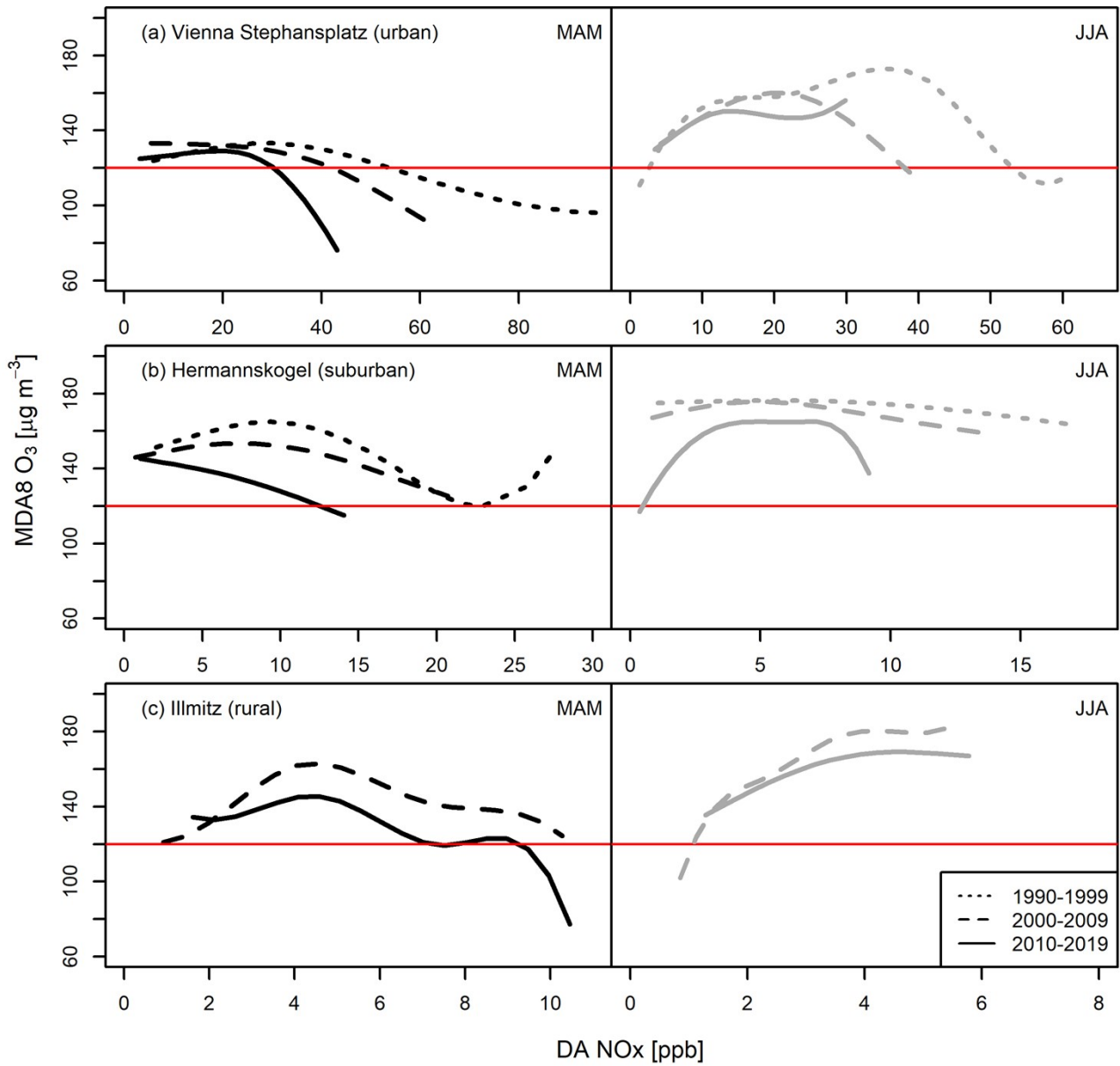
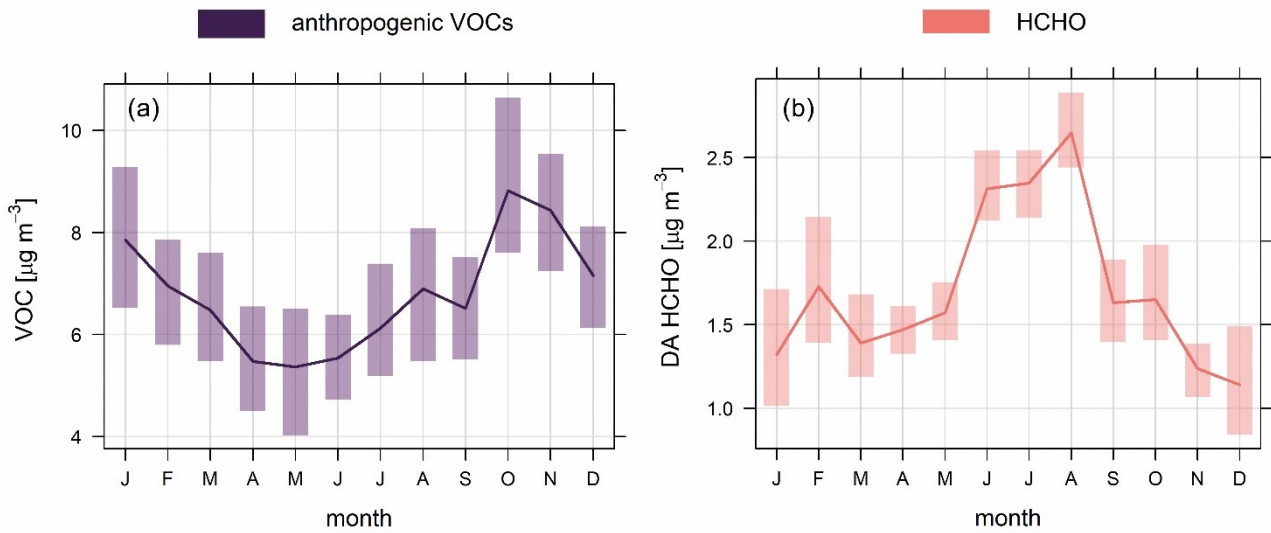


Figure S3: As figure 5 but for sites Graz (12% of observations NO_x limited in JJA), Klösch and Masenberg.



25 **Figure S4:** Evolution of ambient chemical regimes over time for (a) the urban station Vienna Stephansplatz, (b) the suburban site Hermannskogel, and (c) the rural site Illmitz; in analogy to Figure 5. The splines are calculated as polynomial fits of 4th order to the envelopes of the scatterplots of MDA8 O₃ and DA NO_x for the respective decadal time slices. Note, for the rural site Illmitz the period 1990-1999 is not evaluated as NO_x measurements started only in 1995.



30 **Figure S5:** Annual cycle of (a) the sum of selected anthropogenic VOCs (iso-pentane, 1-pentene, n-pentane, 2-pentene, iso-hexane, n-
 35 hexane, benzene, iso-octane, n-heptane, toluene, n-octane, ethylbenzene, m-xylene, p-xylene, o-xylene, 1,3,5-Trimethylbenzol, 1,2,4-
 trimethylbenzene and 1,2,3- trimethylbenzene) and (b) HCHO in Vienna. Data from (a) are collected during 2017-2019 close to the centre
 of Vienna at the monitoring site AKH. The collection cycle is every 6th day, and samples are analysed by gas chromatography. Data in (b)
 are HCHO data obtained during 2017-2019 by the MAX-DOAS instrument at BOKU Vienna.

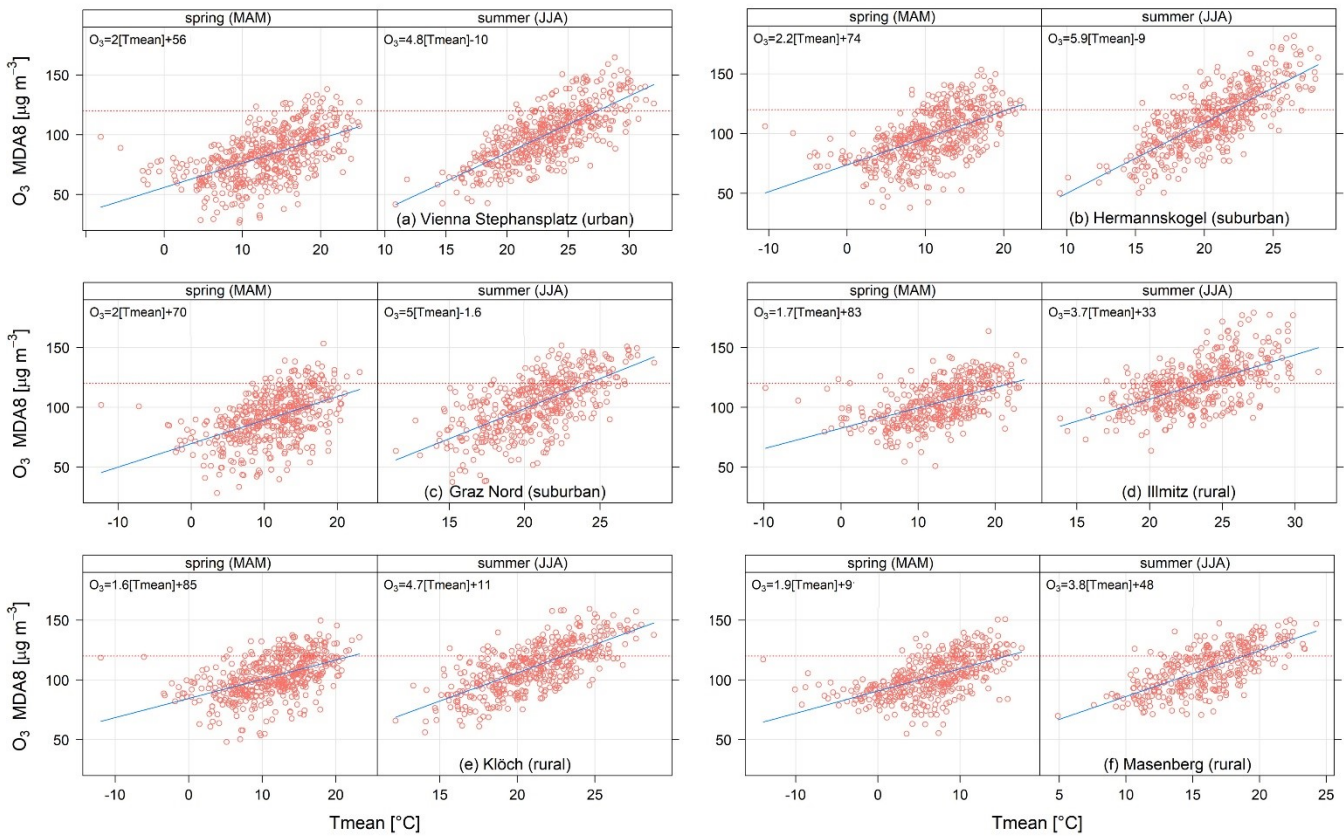


Figure S6: Scatterplots of MDA8 O_3 versus Tmean for (a) the urban station Vienna Center, (b)-(c) suburban sites Hermannskogel, and Graz,
 and (d)-(f) rural sites Illmitz, Klösch, und Masenberg for 20010 – 2019. The red dotted line in all panels indicates the MDA8 target value for
 the protection of human health of $120 \mu\text{g}/\text{m}^3$, blue lines provide linear regression fits.

45

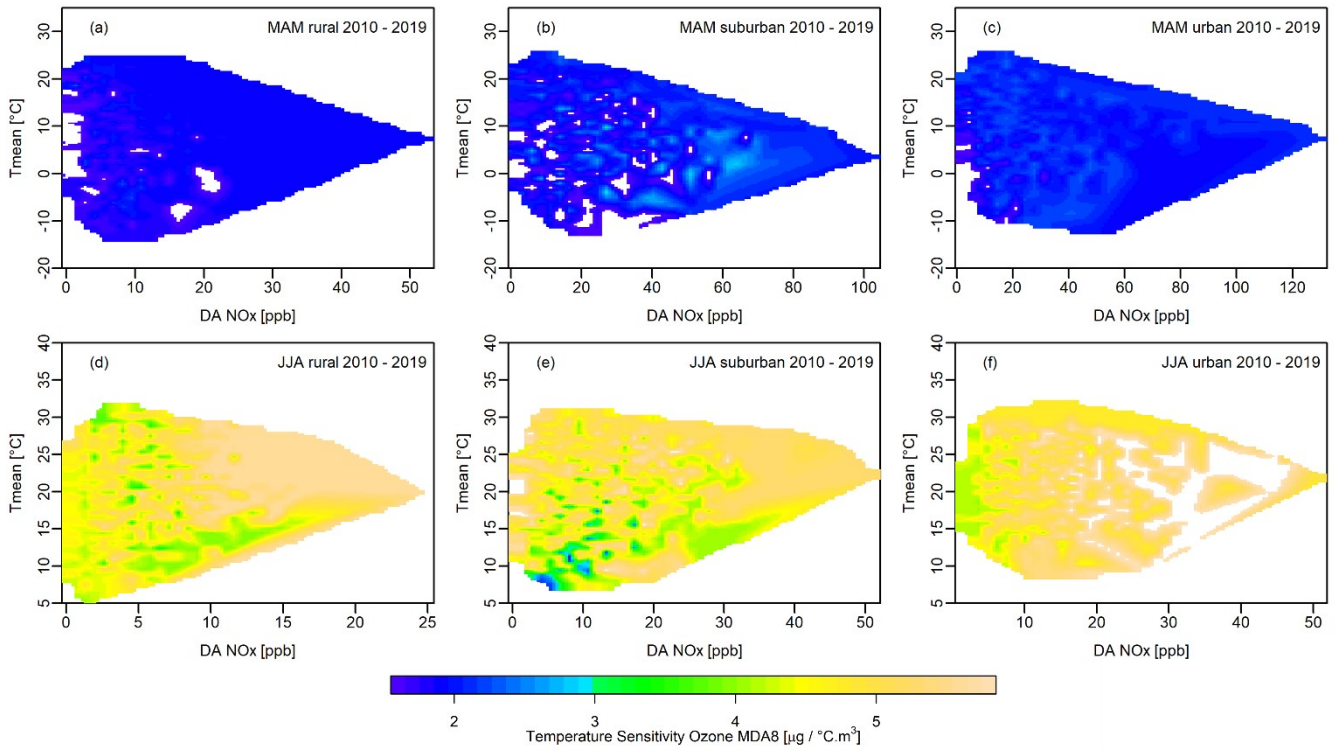


Figure S7: MDA8 ozone temperature sensitivities with respect to Tmean for rural, suburban, and urban monitors for various DA NO_x concentrations and mean temperatures. The ozone temperature sensitivities under clear sky conditions are shown for spring (MAM) in the top panel (a)-(c) and for summer (JJA) in the bottom panel (d)-(f). These data are used to compile the contour plots given in figure 7.

50

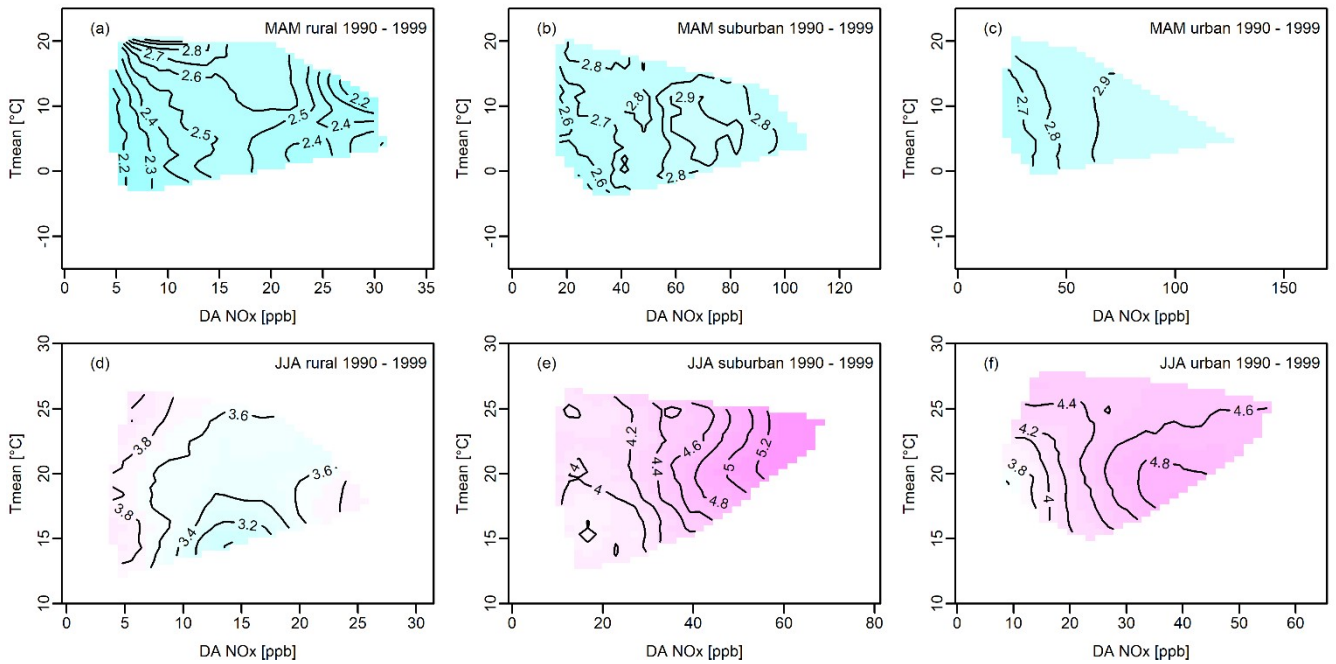


Figure S8: MDA8 O₃ temperature sensitivities with respect to Tmean for rural, suburban, and urban monitors for various DA NO_x concentrations and mean temperatures. The ozone temperature sensitivities for 1990-1999 under clear sky conditions are shown for spring (MAM) in the top panel (a)-(c) and for summer (JJA) in the bottom panel (d)-(f). The contours of the temperature sensitivity of ozone are given in $\mu\text{g}/^\circ\text{C}\cdot\text{m}^3$ with respect to changes of Tmean.

55

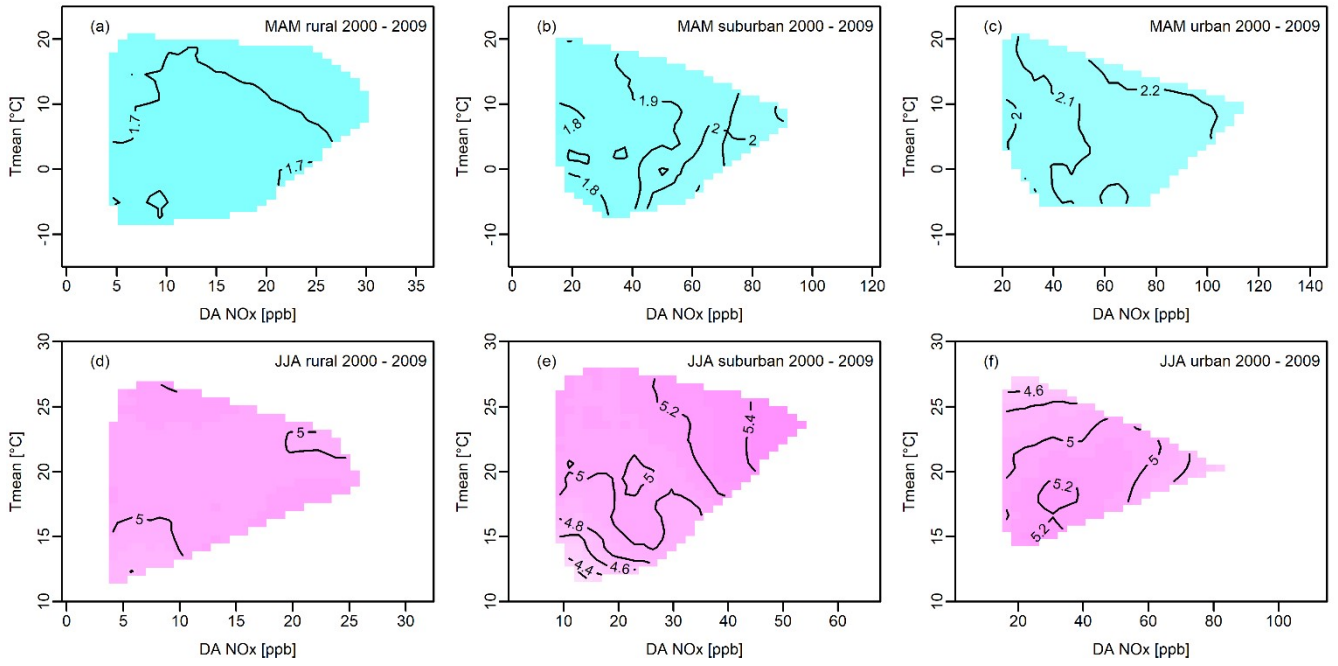


Figure S9: MDA8 O₃ temperature sensitivities with respect to Tmean for rural, suburban, and urban monitors for various DA NO_x concentrations and mean temperatures. The ozone temperature sensitivities for 1990-1999 under clear sky conditions are shown for spring (MAM) in the top panel (a)-(c) and for summer (JJA) in the bottom panel (d)-(f). The contours of the temperature sensitivity of ozone are given in µg/°C.m³ with respect to changes of Tmean.